Intelligent Prediction of FSW Physical Quantity and Joint Mechanical Properties

A method for achieving high-precision prediction of weld tensile strength of aluminum alloy 2219-T8 thick plate is proposed

BY X. H. LU, F. M. ZENG, Y. H. LUAN, AND X. Y. MENG

Abstract

Friction stir welding (FSW) process parameters influence welding temperature field and axial force, which affect welding strength. At present, how the FSW process parameters of aluminum alloy 2219-T8 thick plates influence process physical quantity and how the process physical quantity changes the tensile strength about the welded joint are unknown. We focus on the intelligent prediction of FSW temperature, axial force, and mechanical properties, to provide a basis for FSW process control of aluminum alloy 2219-T8 thick plate. Firstly, we conducted the FSW experiment of aluminum alloy 2219-T8 thick plate. Then, we input the welding process parameters, set up a prediction model by particle swarm optimization-back propagation (PSO-BP) neural network to predict the peak temperature and axial force. Finally, we input the peak temperature and axial force, use genetic algorithm-back propagation (GA-BP) neural network to establish a weld tensile strength estimation model, and comply with the prediction of tensile strength.

Keywords

- Aluminum Alloy 2219-T8 Thick Plate
- FSW
- Intelligent Prediction
- Peak Temperature
- Axial Force
- Tensile Strength
- PSO-BP
- GA-BP

https://doi.org/10.29391/2024.103.002

Introduction

In the last century, aluminum alloy 2219 was used to develop the outer container of the space shuttle with a diameter of 8.4 m; the material has been widely attention since then (Ref. 1). Aluminum alloy 2219 has the characteristics of high strength, good low-temperature resistance, and low sensitivity to welding cracks (Ref. 2). Because of its excellent properties, aluminum alloy 2219 is the preferred material for fuel tank, train carriage, shipbuilding, and automobile manufacturing of spacecraft (Ref. 3). Welding is the main process of aluminum alloy 2219 assembly. In 1991, The Welding Institute developed a new solid-state bonding technique, friction stir welding (Ref. 4). FSW can effectively reduce the deformation and residual stress, reduce the cracks, holes, and other defects in the welding process (Ref. 5). As one of the most effective methods for achieving high strength aluminum welding, FSW improves welding quality.

The main welding process of FSW is as follows: The stirring head rotates and slowly presses into the joint surface of the two welds, and the stirring head rotates in place. Friction heat generation between the stirring head and the weldment and plastic deformation heat generation of the weldment make the material at the weld soften fully. Then the stirring head moves along the welding direction while rotating, the shoulder creates downward pressure while preventing the spillover of softened metal, under the heat-mechanical interaction, the base material is constantly stirred by the stirring head to form a dense combination. After cooling, a solid weld is formed to realize the connection of aluminum alloy materials (Ref. 6).

In the whole welding process of FSW, rotational speed and welding speed affect peak temperature and axial force (Refs. 7–9). The peak temperature distribution and the magnitude of the axial force affect tensile strength of the welded joint (Refs. 10, 11). The peak temperature and axial force affect the stress and strain of the welded joint region, and the temperature variation in the welded joint area is an obvious indicator to observe the plastic deformation degree of metal materials (Refs. 12, 13). Therefore, effective prediction of welding

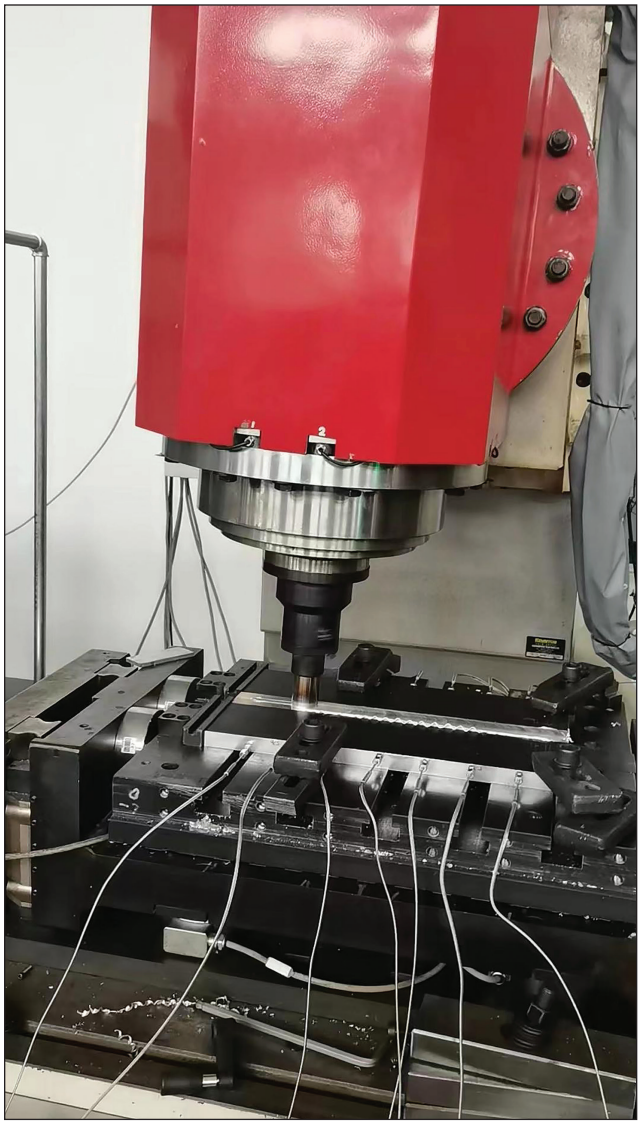

Fig. 1 — Friction stir welding machine.

temperature, axial force, and tensile strength of the welded joint is the key to ensure welding quality. However, in the FSW process, there are complex coupling effects among welding process parameters, peak temperature, axial force, and tensile strength, which leads to difficulty in characterizing the correlation among them.

Some scholars have applied neural network intelligent algorithm to study the application of FSW process, Manvatkar et al. (Ref. 14) adopted the Bayesian method to establish five artificial neural network models, calculated the peak temperature, transverse force, torque, bending stress, and maximum shear stress experienced by the tool in the AA 7075 friction stir process. Input welding variables including shoulder radius, tool speed, pin radius and pin length, welding speed and axial force, tool peak temperature, total torque, transverse force, bending stress, and maximum shear stress as outputs. The forecast error of peak temperature is –7.5 to 7.5%, the predicted errors of total torque, transverse force, bending stress, and maximum shear stress are –12–12%. D'Orazio et al. (Ref. 15) set up a multivariate empirical model based on artificial neural network, the neural network consists of four input parameters (rotational speed, welding speed, speed to welding speed ratio, and processing time) as input layer, the output layer takes vertical force as output, its forecast error is within –5 to 5%. Ghetiya et al. (Ref. 16) conducted FSW experiments on AA8014 plates with a thickness of 4 mm, established the prediction model of tensile strength of the welded joint based on BP neural, the margin of error is within 3%. Wang et al. (Ref. 17) obtained the test data in the process of low-cycle fatigue experimental study on the 5 mm thick 7075-T651 aluminum alloy FSW joint, used the artificial neural network BP algorithm to estimate fatigue life about the welded joints, the margin of error ranges from 0.27 to 5.33%. Padmanaban et al. (Ref. 18) performed dissimilar welding on 5-mm-thick AA2024 and AA7075 plates, measured the joint tensile strength under the different tool speeds and welding speeds, established a model by response surface methods, predicted the tensile strength by the particle swarm optimization algorithm optimize process parameters, and final error between the predicted value and the actual value is within 5%. Alkayem et al. (Ref. 19) used the PSO algorithm for single objective and multiobjective optimization of tensile strength, elongation, and microhardness, and verified the predicted values through experiments, the percentage error ranges from 0.29 to 1.98%. Zhang (Ref. 20) carried out tensile test of FSW joint on 4-mm-thick 6005A-T6 aluminum alloy sheet, used the measured tensile strength and elongation as the data for SVM training and prediction, combined with MATLAB programming, established a relatively new prediction model of friction stir welding joint mechanical properties by support vector machine, put stirring head speed and welding speed as input, realized the prediction of mechanical properties of FSW joint. Verma et al. (Ref. 21) performed dissimilar welding on 6-mm-thick AA6083 and AA8011 plates, put rotational speed, traverse speed, and inclination angle as input, put tensile strength and grain size as output, predicted the performance of friction stir treated joints by using support vector machine (SVM), the error is about 10%.

In the neural network above, the BP and PSO have high prediction accuracy. Some studies have also shown (Refs. 22, 23) that when the output is multiple, the BP neural network optimized under the PSO has good prediction ability and better network performance. In addition, by improving and optimizing the genetic algorithm through global search, the established GA-BP neural network has higher estimate accuracy (Ref. 24).

Through the above analysis, the intelligent algorithm has a good application advantage in FSW. However, the intelligent prediction and control of welded joint performance of aluminum alloy 2219 thick plate is still in the exploration stage. In the welding process, due to the increase of plate thickness, the axial force required for welding increases sharply, and the welding temperature distribution in the direction of welding thickness becomes more uneven, which induces the decrease of tensile strength about welded joints. Therefore, effective prediction of welding temperature, axial force, and post-weld tensile strength can ensure welding quality. Therefore, we establish the prediction model of the peak temperature and axial force, and the prediction model of the weld tensile strength. We propose a new method to predict weld tensile

Table 1 — Chemical Compositions of 2219 Aluminum Alloy (wt-%)

Cu	Mn	Fe	Si	Zn	V	Ti	Zr	Mg	Al
6.21	0.29	0.12	0.15	0.06	0.08	0.03	0.12	0.02	Bal.

Table 2 — Mechanical Properties of 2219 Aluminum Alloy Base Material

Tensile Strength R_m (MPa)	Yield Strength $R_{p0.2}$ (MPa)	Percentage Elongation after Fracture A (%)	Microhardness (HV)
435	405	5.3	142

strength, which is of great significance to welding quality improve.

FSW Experiment of Aluminum Alloy 2219 Thick Plate

The experiment is conducted on the friction stir welding machine tool of Shanghai Top Numerical Control Technology Co. Ltd., as shown in Fig. 1. The shoulder radius of the FSW joint tool is 16 mm, tool pin length is 17.8 mm, and radius of the tool pin is between 3.5 mm and 7.5 mm. The tool pin has a left-handed thread. Using a machine tool with the German HBM company C2 series force sensor, the measuring range of the axial force is 0–400 kN; it provides measurement means for establishing data sets of temperature, axial force, and weld tensile strength in the welding area. Clean welds with alcohol before welding to keep the surface of welds clean.

The material used in the test is aluminum alloy 2219-T8, it is Al-Cu-Mn high strength aluminum alloy, the heat treatment process is cold processing after solid solution treatment, and then artificial aging. and the plate size is 300 × 150 × 18 mm (length × width × thickness). Table 1 shows the analysis of chemical composition by X-ray fluorescence spectrometer (XRF-1800). Table 2 shows the analysis of the mechanical properties of the base metal by electronic universal testing machine DNS-300.

Figure 2 shows the FSW morphology of 2219-T8 aluminum alloy. After welding, we cut two kinds of tensile specimens from 18-mm-thick FSW joint, we first cut it vertically along the seam layer with a thickness of 6 mm, as shown in Fig. 3A; the other is cut along the weld section direction, including a complete weld structure, the thickness is 6 mm, as shown in Fig. 3B. According to GB/T 228.1—2021, metal materials at room temperature tensile test method to determine the sample size. We used the electronic universal testing machine DNS-300 for tensile tests. Figure 4 shows the macro fracture morphology of the joint.

We use the temperature field distribution detection system of FSW based on a multichannel K-type thermocouple developed by the research group, realize the temperature measurement during the welding process. The system has a resolution of 0.1°C, and the test accuracy is 2.5°C. We select different welding parameters (rotational speed and welding speed) for FSW experiments. The installation position of the thermocouple in the workpiece is shown in Fig. 5. A_1, A_2, A_3, A_4, A_5 are the temperature measurement point selected on the forward side of workpiece welding. R_1, R_2, R_3, R_4, R_5 are the temperature measurement point selected on the backward side of workpiece welding. During welding, temperature changes on the forward side and backward side of the selected weld feature points were measured to obtain the welding temperature required for the establishment of the prediction model.

Prediction of Peak Temperature and Axial Force by PSO-BP Neural Network

Through the FSW experiment of aluminum alloy 2219-T8 thick plate, gain various process parameters, physical quantities during welding, and tensile strength data. The peak temperature and axial force are affected by welding parameters in the welding process. Therefore, the establishment of the correlation model between the peak temperature, axial force, and the process parameters will provide a basis for the regulation of welding process parameters. The PSO-BP has high prediction accuracy in multiobjective optimization. Therefore, we predict peak temperature and axial force by PSO-BP neural network.

Determination of PSO-BP Neural Network Structure

BP neural network automatically learns and stores data without specifying the function between input and output in advance, and has no limitation on the number of inputs and output about the prediction model, often used in multivariable coupled process systems. The input layer, hidden layer, and output layer constitute the complete BP neural network. Figure 6 depicts the general structure of the BP neural network. There is a nonlinear continuous transfer function in the hidden layer, so that the nodes in the hidden layer can transmit information like the neurons in the human brain, the

Fig. 2 — Friction stir welding weld morphology of 2219-T8 aluminum alloy.

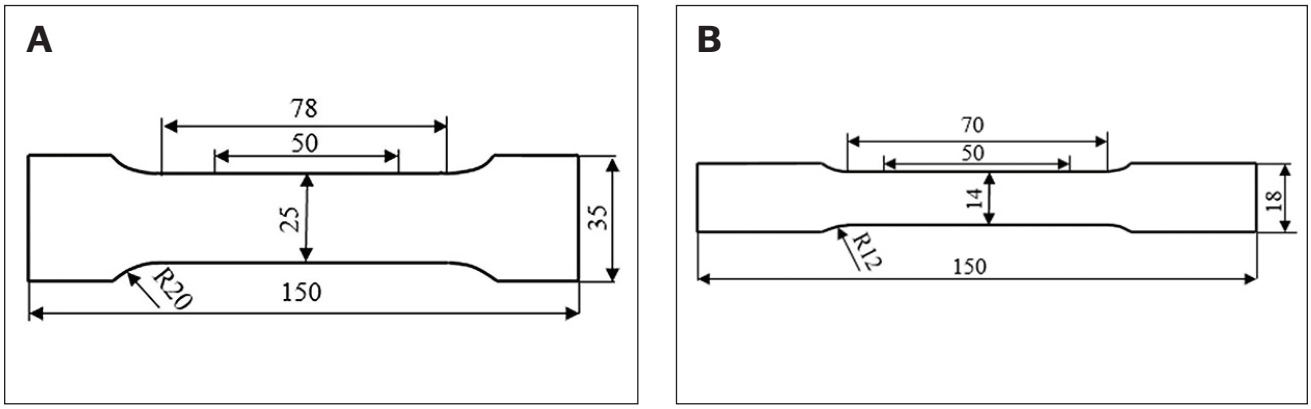

Fig. 3 — Schematic diagram of tensile specimen: A — Vertical weld direction; B — weld section direction.

neural network has the learning ability. BP neural network is a feed forward neural network and it has strong flexibility.

Figure 6 shows that the input data X_1, X_2, L, X_n, O_1, O_2, L, O_m are the predicted value of network output. w_{ij}, w_{jk} represent the connection weights between different layer structures. a_{ij}, b_{ij} indicate the threshold between layer structures.

$$l = n - 1 \tag{1}$$

$$l = \sqrt{m + n} + r \tag{2}$$

$$l = \log_2 n \tag{3}$$

where r is any constant between 0 and 10; n and m are input layer and output layer node; and n and m are related to experimental data. l is the number of hidden layer nodes (Ref. 25).

The PSO algorithm initializes the particle swarm with velocity and position in the solution space to simulate foraging birds. Each particle corresponds to a fitness value and represents a potential solution. How fast a particle moves depends on its speed, and how far it moves depends on its position. Particles move within the potential solution space, updating individual and population speeds and positions through individual and population extremes. The particle is updated every iteration, and the corresponding individual extreme value and population extreme value will also be adjusted until the optimal individual is found. At present, this algorithm has been widely used in data fitting, intelligent control, network optimization, and other fields.

We use the three-layer BP neural network structure with a single hidden layer to accurately predict the peak temperature and axial force of FSW of aluminum alloy 2219-T8 thick plate. Input is welding process parameters, and the peak temperature and axial force are used as the output predictive value. Thus, it can be determined that the number of nodes in both the input layer and output layer is 2.

The nodes in the hidden layer structure of the BP neural network influence output. If there are too many, it will lead to longer running times, the work efficiency will be reduced, and the network will be overfitting. If there are too few, the neurons in the network become less able to learn, and the training accuracy cannot be guaranteed, which results in underfitting. Since the input layer node about the BP neural network FSW peak temperature estimation model is 2, the output layer node is 2. According to the formula (1), (2), and (3), the range of hidden layer nodes is 1–12. Therefore, Fig. 7 represents the structure of BP neural network peak temperature and axial force prediction model by PSO.

Prediction Model of Peak Temperature and Axial Force Based on PSO-BP Neural Network

Table 3 shows the peak temperature and axial force measured in the FSW experiment of aluminum alloy 2219-T8 thick plate.

Table 3 — Peak Temperature and Axial Force of Various Process Parameters

Group	Rotational Speed (r/min)	Welding Speed (mm/min)	Peak Temperature (°C)	Axial Force (kN)
1	300	50	529.2	50.2
2	300	75	522.9	48.6
3	300	100	500.9	45.4
4	300	125	521.6	57.4
5	300	150	499.7	51.2
6	300	175	491.0	52.1
7	350	50	519.8	53.3
8	350	75	517.5	43.4
9	350	100	507.9	42.5
10	350	125	503.9	48.8
11	350	150	495.3	50.1
12	350	175	483.6	60.1
13	400	50	522.2	53.6
14	400	75	531.9	42.3
15	400	100	525.3	46.6
16	400	125	508.2	45.1
17	400	150	504.6	36.1
18	400	175	499.3	40.5
19	420	100	527.5	44.4
20	450	50	515.3	35.9
21	450	75	512.3	40.5
22	450	100	506.8	43.4
23	450	125	501.5	47.2
24	450	150	497.8	45.3
25	450	175	485.1	46.2
26	460	70	510.6	31.5
27	480	65	519.8	37.2

Table 3 — continued

Group	Rotational Speed (r/min)	Welding Speed (mm/min)	Peak Temperature (°C)	Axial Force (kN)
28	480	75	498.3	36.6
29	500	75	509.1	32.4
30	500	85	493.7	33.5

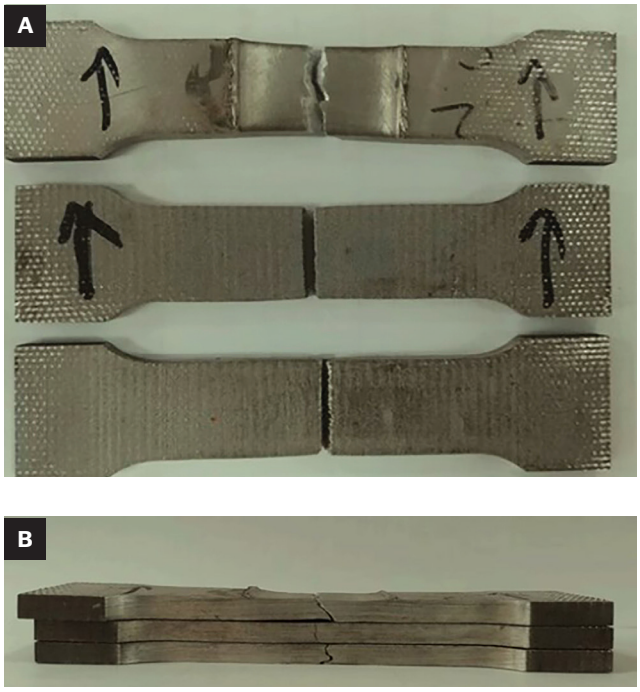

Fig. 4 — Macro fracture morphology of the joint. A — Top view of fracture location; B — fracture section.

The steps for constructing the prediction model of peak temperature and axial force by the PSO-BP neural network are as follows:

1. Input peak temperature and axial force data into the neural network model.

2. Create a batch of particle swarm needed by the model, and randomly assign to this group of particles forward speed and position in the solution set of possible solutions. The particle members will get their own extremum p_{best}, and the whole will have extremum G_{best}.

3. Modify the velocity and direction of the particle members, as follows:

$$V_{id}^{t+1} = \omega V_{id}^{t} + c_1 r_1 (P_{id}^{t} - X_{id}^{t}) + c_2 r_2 \left(P_{gd}^{t} - X_{id}^{t}\right) \quad (4)$$
$$d = 1,2,\ldots,D$$

$$X_{id}^{t+1} = X_{id}^{t} + V_{id}^{t} \quad (5)$$
$$i = 1,2,\ldots,n$$

where w is inertia coefficient; D is solution set dimension; t is the current correction frequency; V_{id} is speed of membership; X_{id} is the direction of progress; c_1 and c_2 are the acceleration coefficient, where $c_1 = c_2 = 1.49$; r_1 and r_2 appear randomly between 0 and 1.

4. According to neuron node connection weights and threshold information contained in each particle, the specific function values of the members are calculated based on BP neural network training error. The following is function value calculation:

$$F = \frac{k}{\sum_{i=1}^{m} abs(y_i - o_i)} \quad (6)$$

The proportional coefficient is k; the experimental value of the i output node is y_i; and the predicted value of the i output node is o_i.

5. When the iteration stops, the optimal individual calculated by the algorithm is passed to BP neural network, giving required connection weights and thresholds to network.

6. Input peak temperature and axial force data to predict (Refs. 26, 27).

GA does not have selection, crossover, and mutation processes, and the speed of the algorithm is relatively fast. Therefore, according to the above steps, set the number of particle swarm to 10, and the number of iterations to 20. Figure 8 exhibits the flow chart of peak temperature and axial force prediction by PSO-BP neural network.

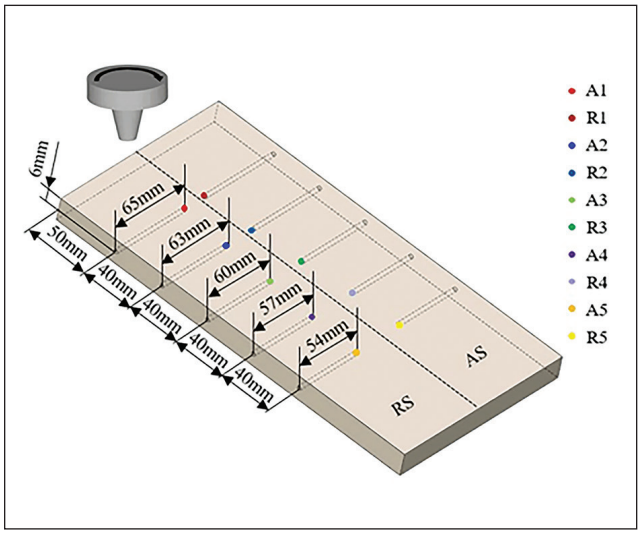

Fig. 5 — Location of thermocouple distribution.

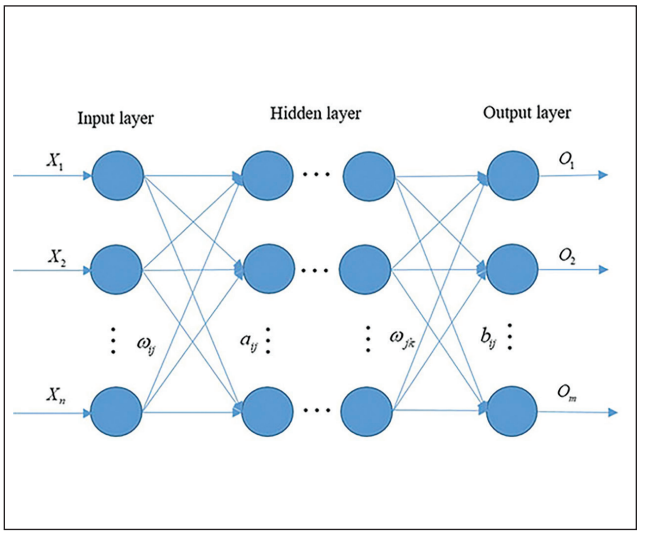

Fig. 6 — BP neural network general structure.

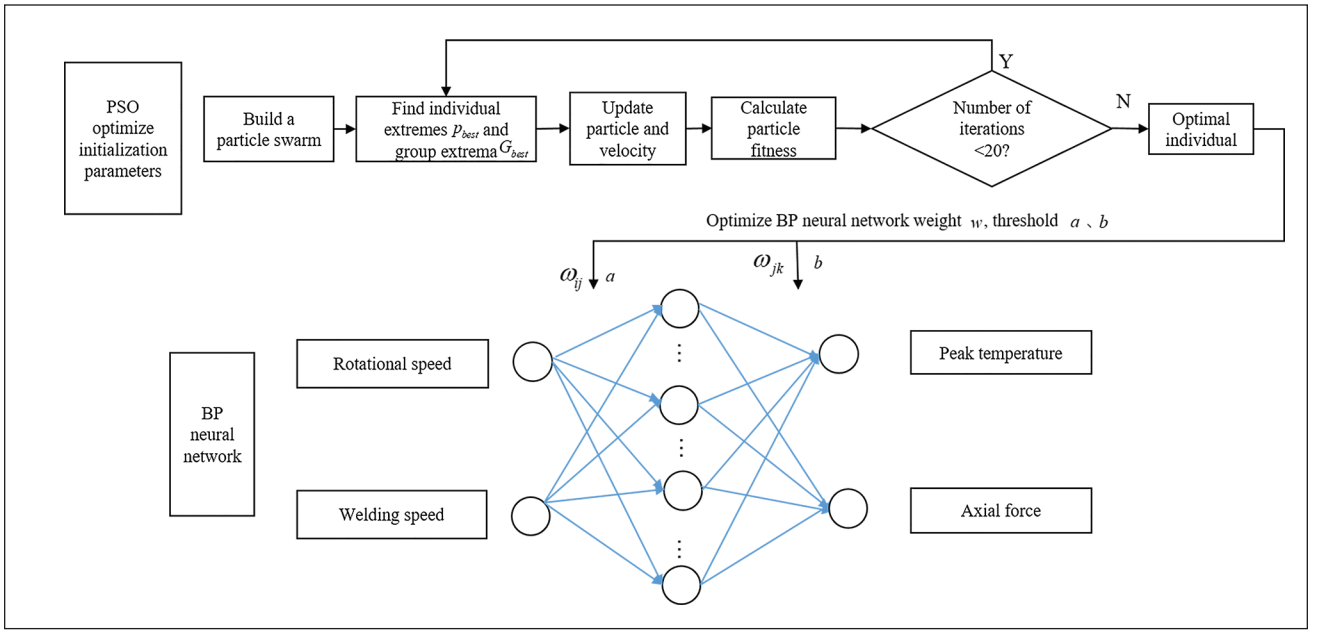

Fig. 7 — Prediction model of peak temperature and axial force based on PSO-BP neural network.

Prediction Results and Discussion of Peak Temperature and Axial Force

We used PSO-BP neural network to build the dual-objective estimation model for peak temperature and axial force of 18-mm-thick 2219-T8 aluminum alloy. Using the experimental data in Table 3, 20 groups of experimental data are extracted randomly to establish a dual-objective prediction network for peak temperature and axial force, so that it can learn and predict. The remaining 10 groups of experimental data verify the accuracy of the network created. Figure 9 reveals the fitness curve. The fitness value does not change after four iterations. PSO algorithm transmits the best individual to the BP neural network for network training.

Figure 10 illustrates the contrast between model output and experimental values. Overall, the predicted values about the peak temperature and the axial force are in keeping with the experimental values. There is no overfitting or underfitting phenomenon. Figure 11 illustrates the prediction error about the established estimation model of peak temperature and axial force by the PSO-BP neural network. The maximum relative error of peak temperature is 2.9%, the average relative error is 1.2%. The maximum relative error of axial force estimation is 10.3%, the average relative error is 5.4%. Therefore, the established prediction model about peak temperature and axial force by the PSO-BP neural network is effective.

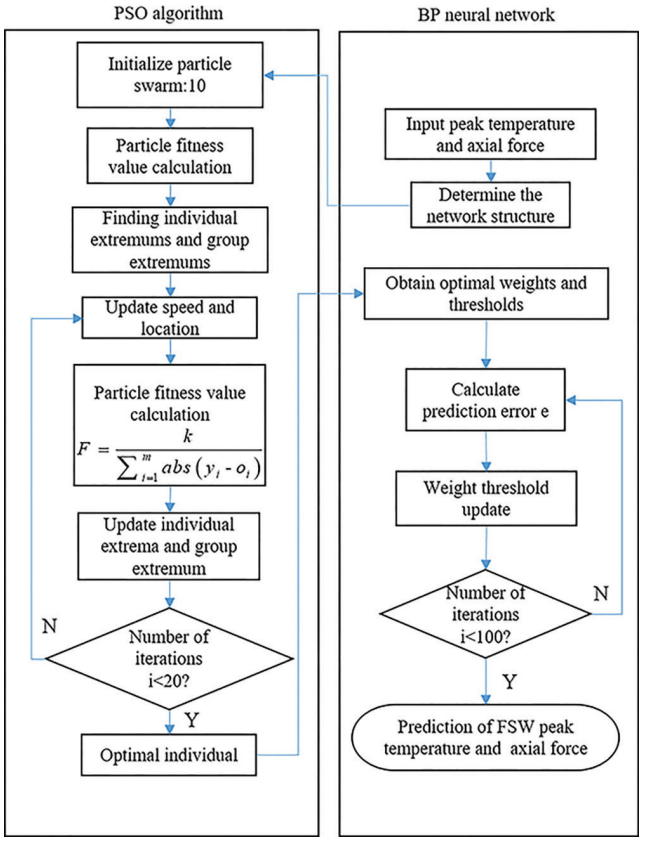

Fig. 8 — Prediction process of peak temperature and axial force based on PSO-BP neural network.

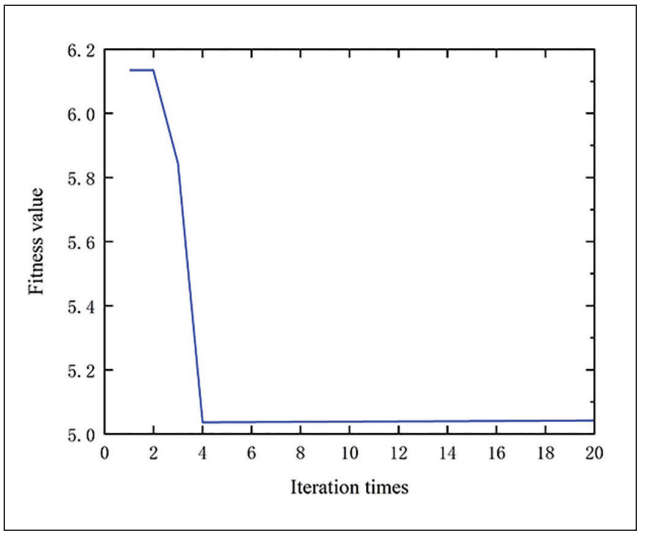

Fig. 9 — Variation curve of fitness value.

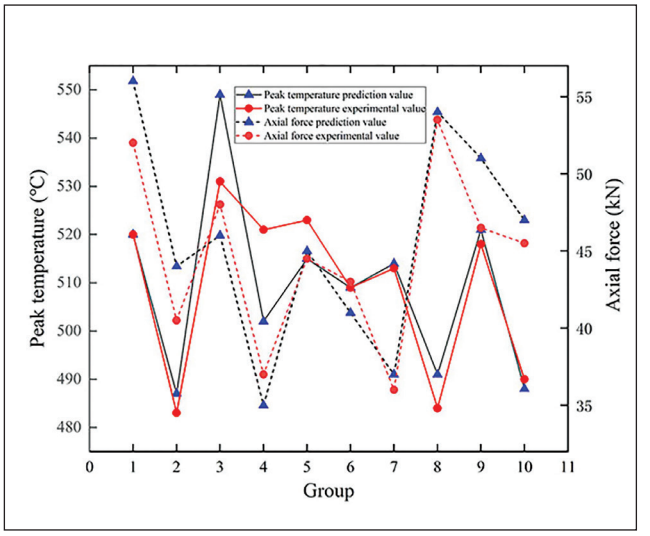

Fig. 10 — Comparison of model prediction results.

Prediction of Tensile Strength Based on GA-BP Neural Network

In the FSW process, different welding process parameters affect welding temperature and axial force, the welding temperature and axial are important factors influencing the tensile strength of the weld. Therefore, we establish the relationship model between welding peak temperature, axial force, and tensile strength, and propose a new method to predict weld tensile strength, which is important for welding quality control. After the genetic algorithm optimized the BP neural network, the performance of the model is greatly improved. We establish a prediction model of weld tensile strength based on the GA-BP neural network.

Determination of GA-BP Neural Network Structure

GA is a global optimization method that simulates biological genetic mechanisms and evolution in nature. It introduces the biological evolutionary principle of survival of the fittest in nature into the algorithm, encodes the initial population information, and uses the fitness function to calculate the fitness value of everyone in the population, through chromosome selection, crossover and mutation, individual genes, and fitness values in the population change. Individuals with better fitness values are retained and transferred to the next generation, while those with poor fitness values are eliminated. The new population formed after one iteration will inherit the information of the previous generation and be superior to the previous generation, and iterate repeatedly until the optimal individual is found. All the components of GA algorithm include running parameters, chromosome coding, fitness function, and genetic manipulation. GA has the characteristics of global optimization. After global optimization, the optimal region is searched, and optimal connection weights and thresholds are obtained by the BP neural network so that the tensile strength of a welded joint can be predicted more accurately based on the optimized BP neural network. GA optimization weight and threshold principle is to use the selection, crossover, and mutation operation of genetic algorithm, through the algorithm iteration update to find the optimal connection weight between each neuron of BP neural network and the threshold of each neural node.

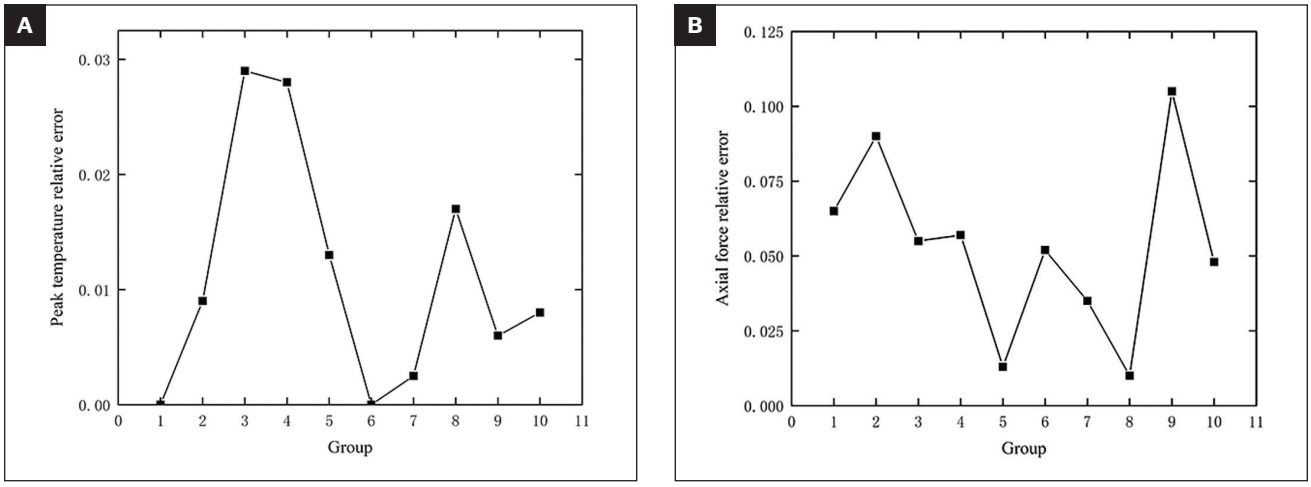

Fig. 11 — Prediction error of peak temperature and axial force by PSO-BP neural network. A — Peak temperature relative error; B — axial force relative error.

The population individuals set by the algorithm carry all the weight and threshold information required by a neural network. The individuals calculate the fitness value through the fitness function, and the GA finds the individuals containing the best fitness value through genetic manipulation. In the prediction part of the BP neural network, the optimal individual obtained by GA is used to assign the initial connection weight and threshold value between each neuron node of the network, and the network reads the input temperature data for training, and then the prediction function can be realized.

First, we edit the initial connection weights and thresholds about the BP neural network under the genetic algorithm to gain the optimal population of individuals. Then the BP neural network adjusts the connection weights and thresholds through the best individual. Then, the tensile strength of the welded joint is predicted based on the GA-BP neural network. Figure 12 illustrates the structure of the GA-BP neural network for the tensile strength of the FSW joint.

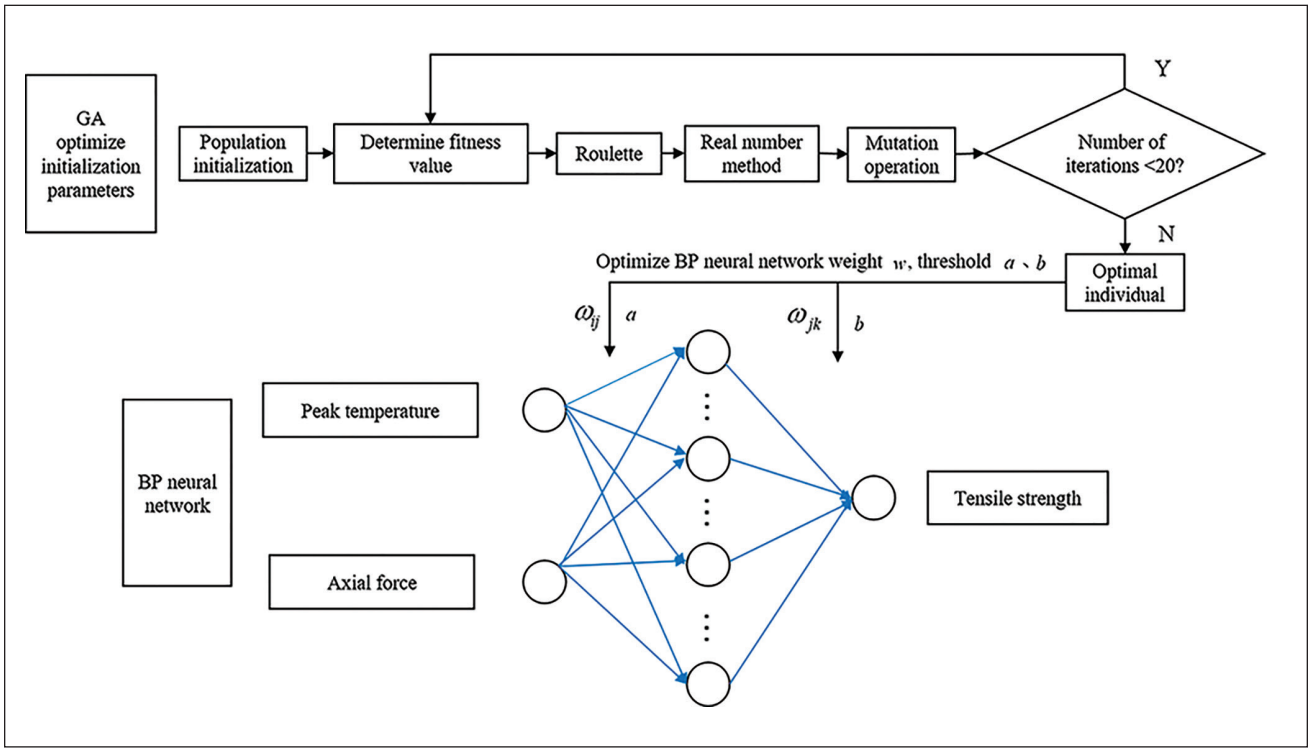

Fig. 12 — Structure of tensile strength prediction model based on GA-BP neural network.

Table 4 — Peak Temperature, Axial Force, and Tensile Strength

Group	Peak Temperature (°C)	Axial Force (kN)	Tensile Strength (MPa)
1	522.9	48.6	303.7
2	522.9	48.6	308.4
3	500.9	45.4	310.0
4	500.9	45.4	303.1
5	521.6	57.4	322.5
6	521.6	57.4	328.9
7	517.5	43.4	319.1
8	517.5	43.4	271.4
9	507.9	42.5	313.4
10	507.9	42.5	291.3
11	503.9	48.8	323.6
12	503.9	48.8	293.2
13	531.9	42.3	299.9
14	531.9	42.3	287.8
15	525.3	46.6	316.4
16	525.3	46.6	337.3
17	508.2	45.1	327.4
18	508.2	45.1	288.8
19	512.3	40.5	299.1
20	512.3	40.5	265.5
21	503.8	43.4	296.3
22	503.8	43.4	304.7
23	501.5	47.2	309.4
24	501.5	47.2	317.8

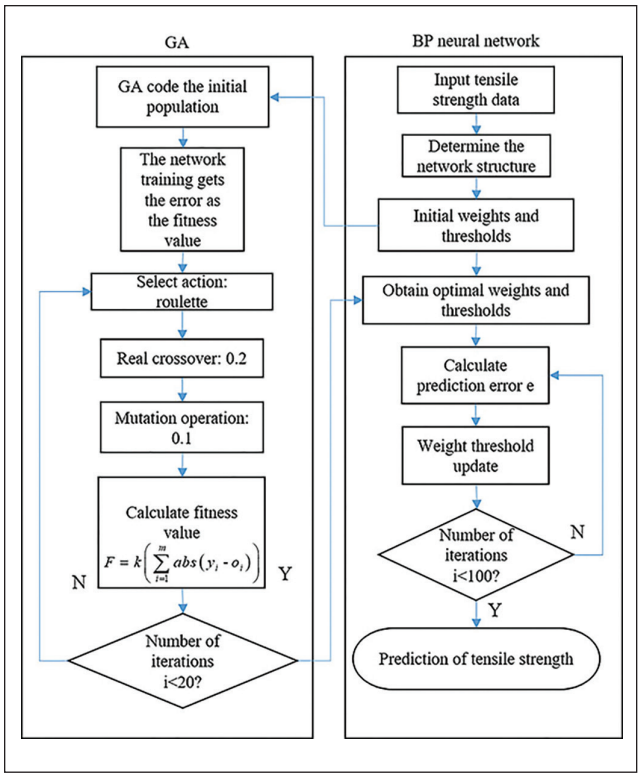

Fig. 13 — Prediction model of tensile strength of FSW joint based on GA-BP neural network.

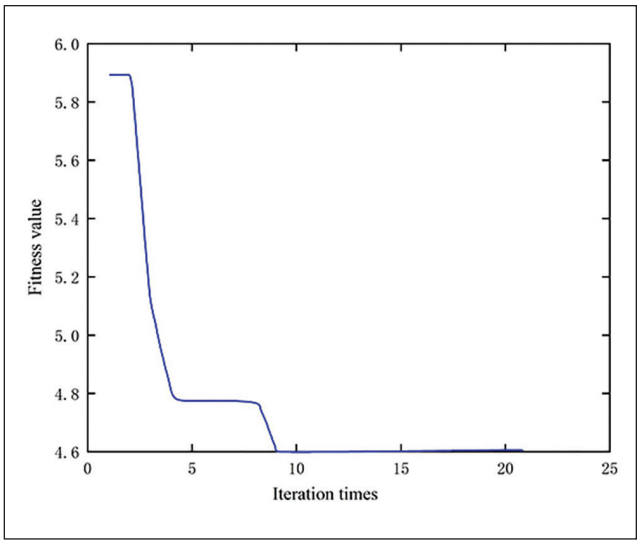

Fig. 14 — Variation curve of fitness value.

Prediction Model of Tensile Strength Based on GA-BP Neural Network

To have enough data to train the model to ensure accuracy, we performed a series of tensile experiments. Table 4 exhibits experimental data about peak temperature, axial force, and tensile strength of welded joints.

The tensile strength prediction model established by GA-BP was obtained by the following steps:

1. Train tensile strength data in Table 4 by GA-BP neural network model.

2. Build the initial population, population size set to 20, and use real coding. The coding length is operated based on the following formula:

$$L = n \times l + l \times m + l + m \tag{7}$$

3. The fitness function value of training error about BP neural network is calculated by the following formula:

$$F = k\left(\sum_{i=1}^{m} abs(y_i - o_i)\right) \tag{8}$$

where proportional coefficient is k, predicted value of the first output node of the neural network is y_i, predicted value of the i output node is o_i.

4. The probability p_i of each i selected by the roulette method is operated by the following formula:

$$f_i = \frac{k}{F_i} \tag{9}$$

$$p_i = \frac{f_i}{\sum_{j=1}^{N} f_i} \tag{10}$$

where fitness value of individual i is F_i, population number is N.

5. Chromosome genetic information is crossed by real numbers, and the genetic information of the k chromosome a_k and the l chromosome a_l after crossing at j position is as follows:

$$\begin{cases} a_{kj} = a_{kj}(1-b) + a_{lj}b \\ a_{lj} = a_{lj}(1-b) + a_{kj}b \end{cases} \tag{11}$$

where b appears randomly between 0 and 1.

6. After the last step about the operation, genetic information of the chromosome is mutated with a set probability. The genetic information of the j gene a_{ij} mutation of the i individual as follows:

$$a_{ij} = \begin{cases} a_{ij} + (a_{ij} - a_{max}) \times f(g) & r > 0.5 \\ a_{ij} + (a_{min} - a_{ij}) \times f(g) & r \le 0.5 \end{cases} \tag{12}$$

a_{max} and a_{min} are upper and lower bounds about gene a_{ij}, respectively, $f(g) = r_2(1\text{-}g/G_{max})^2$, r_2 is the random number, g is the modification number, G_{max} is the maximum evolution number, and r appears randomly between 0–1.

7. When the GA loop stops, complete the optimization of the connection weights required.

8. Use trained BP neural network to predict test dates (Refs. 28, 29).

Through the above steps, we optimize the BP neural network, set the population size to 20, the number of iterations

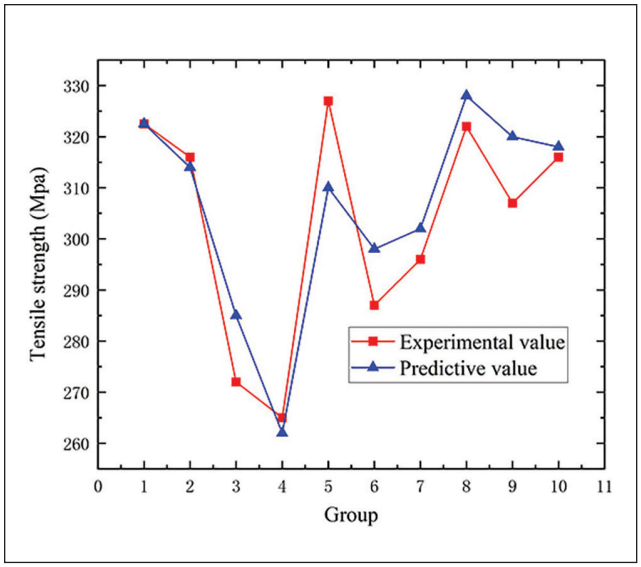

Fig. 15 — Comparison between predicted value and experimental value.

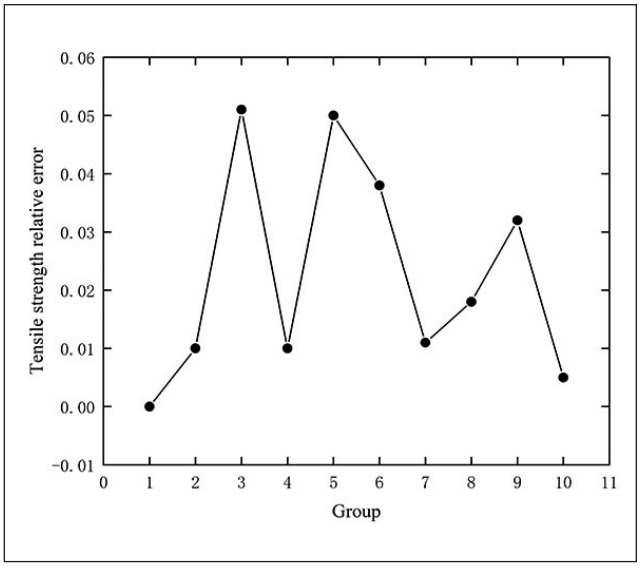

Fig. 16 — Prediction error of tensile strength by GA-BP neural network.

to 20, the crossover probability to 0.2, and the mutation probability to 0.1. Figure 13 shows the prediction process of the FSW joint tensile strength prediction model by the GA-BP neural network.

Prediction Results and Discussion of Tensile Strength

The tensile strength prediction model is established by the GA-BP neural network, using Table 4 axial force, welding peak temperature, and tensile strength data. The training data is obtained by randomly selecting 14 sets of samples from the table, and another 10 sets of data are selected as validation samples to verify the estimation accuracy. After the average fitness value is close to 10 iterations, the fitness value does not change. GA passes the best individual to the BP neural network for network training. Figure 14 reveals the fitness curve.

Figure 15 depicts a comparison between predicted and experimental values. The predictive value is in good agreement with the experimental results, indicating that the curve fits well and there is no overfitting phenomenon, which reflects the great advantage of the GA-BP neural network in predicting tensile strength.

The relative error of the welded joint tensile strength prediction model is shown in Fig. 16. It shows the maximum relative error of FSW joint tensile strength prediction based on the GA-BP neural network is 5.2%, average relative mistake is 2.3%. Thus, the GA-BP neural network is used to realize high-precision prediction of weld tensile strength.

Conclusions

Aiming at the aluminum alloy 2219-T8 thick plate FSW morphic characteristic detection problem, we conducted the FSW experiment of 18-mm-thick aluminum alloy 2219-T8, combined the material structure theory and neural network intelligence algorithm, and established a prediction model of physical parameters (temperature and axial force) and tensile strength of aluminum alloy 2219-T8 thick plate during FSW. Through these two models, we have realized the prediction of FSW temperature, axial force, and tensile strength of aluminum alloy 2219-T8 thick plate, and provide a practical method for the implementation of predictive control. The research content includes the following two aspects:

1. Based on the temperature measurement experimental data of FSW, we take the rotational speed and welding speed of tool as input parameters, the FSW peak temperature and axial force as output parameters, build a prediction model of the peak temperature, and the axial force by the PSO-BP neural network. The maximum relative error about the peak temperature is 2.9%, and the average relative error is 1.2%. The maximum relative error for axial force prediction is 10.3%, and the average relative error is 5.4%. Confirm that the established prediction model of peak temperature and axial force by the PSO-BP neural network is effective.

2. Based on the data of peak temperature, axial force, and tensile strength of the joint, we take the FSW peak temperature and axial force as input parameters, the tensile strength of welded joint as output parameters, and establish an estimation model about the tensile strength based on GA-BP neural network. The maximum relative error is 5.2%, and the average relative error is 2.3%, achieving high-precision prediction of weld tensile strength.

Acknowledgments

The research was supported by the National Key Research and Development Program of China (Grant No. 2019YFA0709003) and Natural Science Foundation of Liaoning Province of China (2023-MS-101). The financial contributions are gratefully acknowledged.

References

1. Liu, C. F. 2003. Material selection for new-type launch vehicle tank. *Aeronautical Manufacturing Technology* (2): 22–27. DOI: 10.3969/j.issn.1671-833X.2003.02.009 In Chinese

2. Qu, W. Q, Song, M. Y., Yao, J. S., and Zhao, H. Y. 2011. Effect of temperature and heat treatment status on the ductile fracture toughness of aluminum alloy 2219. *Mater. Sci. Forum* 689: 302. DOI: 10.4028/www.scientific.net/MSF.689.302

3. Malarvizhi, S., Raghukandan, K., and Viswanathan, N. 2008. Effect of post weld aging treatment on tensile properties of electron beam welded AA2219 aluminum alloy. ***Int.*** *J. Adv. Des. Manuf. Technol* 37(3–4): 294–301. DOI: 10.1007/s00170-007-0970-7

4. Patel, V., Li, W. Y., Vairis, A., and Badheka, V. 2019. Recent development in friction stir processing as a solid-state grain refinement technique: microstructural evolution and property enhancement. *Crit. Rev. Solid State Mater. Sci* 44(5): 378–426. DOI: 10.1080.10408436.2018.1490251

5. Biswas, P., Kumar, D. A., and Mandal, N. R. 2012. Friction stir welding of aluminum alloy with varying tool geometry and process parameters. *Proc. Inst. Mech. Eng., Part B* 226(B4): 641–648. DOI: 10.1177/0954405411424111

6. Du, Z. Y. 2018. Optimization of friction stir welding process and Study on microstructure and properties of 2219 aluminum alloy biaxial shoulder. *Harbin Institute of Technology.*

7. Zhao, Y., Wu, A. P., Ren, J. L., Sato, Y. S., Kokawa, H., Miyake, M., and Yan, D. Y. 2013. Temperature and force response characteristics of friction stir welding on Invar 36 alloy. *Sci. Technol. Weld. Joining* 18(3SI): 232–238. DOI: 10.1179/1362171812Y.0000000077

8. Papahn, H., Haghpanahi, M., and Bahemmat, P. 2017. Using a novel fixture to study of temperature and applied forces during friction stir welding. *J. Braz. Soc. Mech. Sci. Eng* 39(2): 531–541. DOI: 10.1007/s40430-015-0408-3

9. Nie, L., Wu, Y. X., and Gong, H. 2020. Prediction of temperature and residual stress distributions in friction stir welding of aluminum alloy. *Int. J. Adv. Manuf. Tech* 106(7–8): 3301–3310. DOI: 10.1007/s00170-019-04826-4

10. Lu, X. H., Meng, X. Y., Ma, C., Sun, S. X., and Liang, S. Y. 2022. Microstructure and mechanical properties of FSW medium thickness 2219 aluminum alloy. *Proc. Inst. Mech. Eng., Part C* 236(16): 9072–9080. DOI: 10.1177/095440622210888550

11. Jayaraman, M., Sivasubramanian, R., Balasubramanian, V., and Babu, S. 2009. Optimisation of friction stir welding process parameters to weld cast aluminium alloy A413-an experimental approach. *Int. J. Cast. Metal. Res* 22(5): 367–373. DOI: 10.1179/174313309X380404

12. Zhang, Z. 2019. Temperature predictive control of FSW. Dissertation, Jiangsu University of Science and Technology.

13. Zhao, B. 2016. Analysis of temperature field in friction stir welding based on orthogonal ridgelet finite element method. *J. Therm. Anal. Calorim* 123(2): 1751–1758. DOI: 10.1007/s10973-015-5014-1

14. Manvatkar, V. D., Arora, A., De. A., and Debroy, T. 2012. Neural network models of peak temperature, torque, traverse force, bending stress and maximum shear stress during friction stir welding. *Sci. Technol. Weld. Joining* 17(6): 460–466. DOI: 10.1179/1362171812Y.0000000035

15. D'Orazio, A., Forcellese, A., and Simoncini, M. 2019. Prediction of the vertical force during FSW of AZ31 magnesium alloy sheets using an artificial neural network-based model. *Neural. Comput. Appl* 31(11): 7211–7226. DOI: 10.1007/s00521-018-3562-6

16. Ghetiya, N. D., and Patel, K. M. 2014. Prediction of tensile strength in friction stir welded aluminium alloy using artificial neural network. 2nd International Conference on Innovations in Automation and Mechatronics Engineering, ICIAME 14: 274–281. DOI: 10.1016/j.protcy.2014.08.036

17. Wang, X. J., Xu, C., Zhang, J., Li, S. W., and Niu, Y. 2008. Fatigue life prediction of friction-stir welding joints of aluminum alloy 7070-7651 based on BP algorithm of neural network. *Lanzhou Ligong Daxue Xuebao* 34(3): 12–15. DOI: 10.3969/j.issn.1673-5196.2008.03.004

18. Padmanaban, R., Vignesh, R. V., Povendhan, A. P., and Balakumharen, A. P. 2018. Optimizing the tensile strength of friction stir welded dissimilar aluminium alloy joints using particle swarm optimization. *Mater. Today: Proc* 5(113): 24820–24826. DOI: 10.1016/j.matpr.2018.10.280

19. Sarvaiya, J., and Singh, D. 2022. Selection of the optimal process parameters in friction stir welding/processing using particle swarm optimization algorithm. *2nd International Conference on Engineering Materials, Metallurgy and Manufacturing* (ICEMMM) 62: 896–901. DOI: 10.1016/j.matpr.2022.04.062

20. Zhang, L. G., He, J., and Gao, S. S. 2015. Mechanical property prediction of friction stir welding joint based on support vector machine. *Journal of Shenyang Aerospace University* 33(1): 24–27. DOI: 10.3969/j.issn.2095-1248.2016.01.005

21. Verma, S., Msomi, V., Mabuwa, S., Merdji, A., Misra, J. P., Batra, U., and Sharma, S. 2021. Machine learning application for evaluating the friction stir processing behavior of dissimilar aluminium alloys joint. *Proceedings of the Institution of Mechanical Engineers Part L-Journal of Materials-Design and Applications* 236(3): 633–646. DOI: 10.1177/14624207211053123

22. He, M., Xu, Y., Wang, R., and Hu, S. Z. 2018. Combination dynamic inertia weight particle swarm optimization algorithm to optimize neural network and application. *Computer Engineering and Applications* 54(19): 107–113, 128. DOI: 10.3778/j.issn.1002-8331.1706-0206

23. Gong, Q. J., Guo, Y. B., Chen, H. X., Cheng, Y. H., and Xu, S. M. 2020. Prediction of variable-speed compressor power based on particle swarm optimization and back propagation neural network. *Journal of Refrigeration* 41(1): 89–95. DOI: 0253-4339(2020)41:1<89:JYLZQY>2.0.TX;2-T

24. Yu, F., and Xu, X. 2014. A short-term load forecasting model of natural gas based on optimized genetic algorithm and improved BP neural network. *Appl Energy* 134: 102–113. DOI: 10.1016/j.apenergy.2014.07.104

25. Xiangrong, X. 2021. Prediction of the optimal umbrella shape of insulators based on data mining technology. *IOP Conference Series: Earth and Environmental Science* 692: 22067–22068. DOI: 10.1088/1755-1315/692/2/022067

26. Cao, J., Cui, H., Shi, H., and Jiao, L. J. 2016. Big data: A parallel particle swarm optimization-back-propagation neural network algorithm based on MapReduce. *Plos. One* 11(e01575516). DOI: 10.1371/journal.pone.0157551

27. Kulkarni, N. K., Patekar, S., Bhoskar, T., Kulkarni, O., Kakandikar, G. M., and Nandedkar, V. M. 2015. Particle swarm optimization applications to mechanical engineering - A review. *Mater. Today: Proc* 2(4–5): 2631–2639. DOI: 10.1016/j.matpr.2015.07.223

28. Chen, X. P., Wang, S. L., Xie, Y. X., Fernandez, C., and Fan, Y. C. 2021. A novel fireworks factor and improved elite strategy based on back propagation neural networks for state-of-charge estimation of lithium-ion batteries. *Int. J. Electrochem. Sci* 16(2109489). DOI: 10.20964/2021.08.07

29. Xiao, Q., Wang, R., Zhang, S. J., Li, D. Y., Sun, H. Y., and Wang, L. M. 2020. Prediction of pilling of polyester-cotton blended woven fabric using artificial neural network models. *J. Eng. Fiber. Fabr* 15(1558925019900152). DOI: 10.1177/1558925019900152

XIAOHONG LU (*lxhdlut@dlut.edu.cn*), **FANMAO ZENG, YIHAN LUAN,** and **XIANGYUE MENG** are with the School of Mechanical Engineering, Dalian University of Technology, People's Republic of China.